Disruption of human limb morphogenesis by a dominant negative mutation in *CDMP1*

J. Terrig Thomas[1], Michael W. Kilpatrick[2], Keming Lin[1], Ludwig Erlacher[1], Peter Lembessis[2], Teresa Costa[3], Petros Tsipouras[2] & Frank P. Luyten[1]

Chondrodysplasia Grebe type (CGT) is an autosomal recessive disorder characterized by severe limb shortening and dysmorphogenesis. We have identified a causative point mutation in the gene encoding the bone morphogenetic protein (BMP)–like molecule, cartilage-derived morphogenetic protein–1 (CDMP-1). The mutation substitutes a tyrosine for the first of seven highly conserved cysteine residues in the mature active domain of the protein. We demonstrate that the mutation results in a protein that is not secreted and is inactive *in vitro*. It produces a dominant negative effect by preventing the secretion of other, related BMP family members. We present evidence that this may occur through the formation of heterodimers. The mutation and its proposed mechanism of action provide the first human genetic indication that composite expression patterns of different BMPs dictate limb and digit morphogenesis.

The skeletal elements of the vertebrate limb arise from condensing mesenchymal cell populations. The size and shape of the condensations, together with their growth, branching and segmentation, determine limb pattern. Differentiation of condensed mesenchymal cells into chondrocytes leads to the establishment of cartilaginous precursor elements (anlagen), from which bone subsequently forms by endochondral ossification[1]. One group of signalling molecules known to be intimately involved in cartilage and bone formation are the bone morphogenetic proteins (BMPs), which were originally isolated and characterized from bovine bone matrix by their ability to induce cartilage and bone formation when implanted at an ectopic site[2–4]. They belong to the TGF-β superfamily of multifunctional signalling molecules, which are critically engaged in a variety of developmental processes[5]. BMPs are initially synthesized as monomeric pro-forms, which subsequently dimerize before being cleaved enzymatically at a characteristic R-X-X-R consensus site. The formation of a correctly folded mature secreted dimer is essential for eliciting a biological response upon binding to specific serine-threonine kinase receptors.

Cartilage-derived morphogenetic protein–1 (CDMP-1: OMIM 601146), also termed growth/differentiation factor 5 (Gdf5), is closely related to the BMPs[6,7]. It is expressed predominantly at sites of cartilage differentiation in developing limbs, where it may function as a signal for chondrogenesis[6,7]. In addition, expression of *CDMP1* at the position of future joint spaces suggests a role in the formation of articulations[8]. Studies of naturally occurring null mutations in mice (*bp*)[7] and humans (acromesomelic chondrodysplasia, Hunter-Thompson type (CHTT); OMIM 201250; ref. 9) demonstrate that the development of appendicular skeletal elements and joint morphogenesis are severely perturbed in the absence of CDMP-1.

In an ongoing effort to further define the molecular basis of skeletogenesis, our attention was drawn to chondrodysplasia Grebe type (OMIM 200700; refs 10,11). CGT resembles CHTT in that abnormalities are restricted to the appendicular skeleton. However, the degree of skeletal and joint dysplasia is much more pronounced. We report that CGT is caused by a point mutation in *CDMP1*, resulting in a cysteine-to-tyrosine substitution in the mature protein (CDMP-1^{C400Y}). However, unlike the null mutation[9], *CDMP1*^{C400Y} acts as a dominant negative mutation. We found that the mutated protein is not processed or secreted and prevents the secretion of other BMPs through the formation of non-functional heterodimers.

Chondrodysplasia Grebe type

CGT is an autosomal recessive disorder characterized by severe abnormality of the limbs and limb joints. The severity of limb shortening progresses in a proximal-distal gradient, with the hands and feet being most affected (Figs. 1*a,b,f*). The fingers and toes lack articulation and appear as skin appendages (Fig. 1*b*). In contrast, axial skeletal structures and the craniofacial skeleton, including the temporo-mandibular joint, are not affected. Heterozygous individuals are of average stature and have a variety of mild skeletal abnormalities, including postaxial polydactyly, brachydactyly (Fig. 1*e*), delayed bone age, metatarsus adductus, valgus deviation of toes and flexion contracture of fingers (not shown).

G→A transition in *CDMP1* segregates with CGT

Human *CDMP1* maps to chromosome 20q11.2 and is tightly linked to *D20S191* and *D20S195* (ref. 12). Haplotype analysis with polymorphic $(CA)_n$ repeat markers for *D20S191*, *D20S195* and *CDMP1* demonstrated a common *D20S191*:*D20S195*:*CDMP1* 2:1:1 haplotype in thirteen of fourteen affected chromosomes. The remaining chromosome was detected in an affected individual (Fig. 2, #13) with one copy of the 2:1:1 haplotype and one copy of a 1:1:1 haplotype. All obligate carriers analysed possess one copy of the 2:1:1 haplotype. Affected individuals homozygous for the 2:1:1 haplotype have a G→A transition at nucleotide 1199, predicting a tyrosine for cysteine substitution at amino-acid 400 (C400Y) in the mature region of CDMP-1 (Fig. 3). The G1199A substitution eliminates a *Pst*I restriction site, permitting direct analysis of PCR products flanking the mutation by *Pst*I restriction digestion (Fig. 2). The affected individual with the 2:1:1, 1:1:1 haplotype was found to be a compound heterozygote, possessing one allele for the G1199A mutation and the other for a deletion of a G nucleotide at position 1144, predicting a frameshift and premature stop codon 70 amino

[1]*Craniofacial and Skeletal Diseases Branch, National Institute of Dental Research, National Institutes of Health, Bethesda, Maryland 20892, USA.* [2]*Department of Pediatrics, University of Connecticut Health Center, Farmington, Connecticut 06030, USA.* [3]*Department of Genetics, The Hospital for Sick Children, Toronto, Ontario, Canada. Correspondence should be addressed to J.T.T. e-mail: tthomas@yoda.nidr.nih.gov*

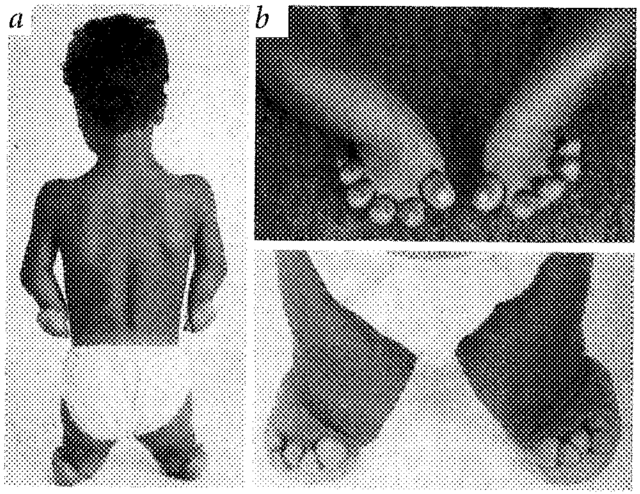

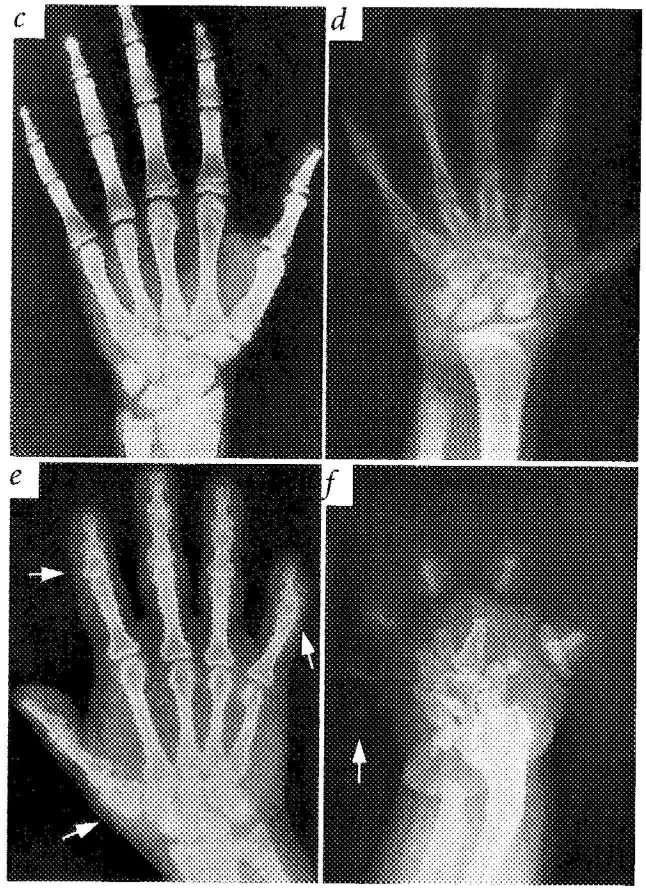

Fig. 1 Clinical and radiographic characteristics of CGT in comparison with CHTT. ***a***, in a 10-year-old CGT-affected boy, abnormalities are restricted to the limbs, with dramatic shortening in a proximo-distal fashion. The range of motion of the elbows, wrists, hands, knees and ankles is either severely restricted or non-existent because of gross skeletal dysmorphogenesis. In contrast, no apparent abnormalities are observed in the acromio-clavicular, sterno-clavicular, or costo-sternal joints, and the craniofacial and axial skeleton is normal. ***b***, Enlarged view of the arms and legs. Five of eight affected individuals presented with postaxial polydactyly of the fifth digit. ***c–f***, Comparison of severity of hand malformations between Hunter-Thompson and Grebe type chondrodysplasia. ***c***, X-ray of a normal hand (age-matched to *d*). ***d***, Homozygous Hunter-Thompson phenotype associated with frameshift mutation and loss of function of CDMP-1 (ref. 10). ***e***, Heterozygous CGT individual (#9 in Fig. 3) showing brachydactyly. Note the very short first metacarpal and second and fifth medial phalanges (arrows). There is clinodactyly of the fifth finger, and the styloid process of the ulna is absent. ***f***, Phenotype of homozygous CGT associated with *CDMP1*^{C400Y} mutation. Note the greater severity of skeletal dysmorphogenesis than in *d*. There is an abnormal shape and a reduced number of carpal bones and apparent fusion of several carpal bones. Note abnormal size, shape or absence of metacarpals and proximal and medial phalanges, and there is one extra distal phalanx (sixth digit). Note shortened and abnormally shaped radius and absence of distal part of the ulna.

acids downstream (Fig. 3). This individual is phenotypically identical to homozygotes for the G1199A mutation. The ΔG1144 mutation was not present in any of the other 1:1:1 haplotypes analysed and may represent a sporadic mutation. Affected individuals in the three unrelated families were also found to be homozygous for the C400Y mutation (not shown).

CDMP-1^{C400Y} is not secreted or biologically active

The effect of the *CDMP1*^{C400Y} mutation on the synthesis and secretion of CDMP-1 was determined by western analysis of cell extracts and culture supernatants of COS-7 cells transfected with *CDMP1* or *CDMP1*^{C400Y}. Analysis of cell extracts after *CDMP1* transfection demonstrated the presence of unprocessed as well as small amounts of processed mature CDMP1 (Fig. 4*a*). In the culture supernatant, CDMP-1 was secreted only as a mature processed form. In contrast, although cell extracts from *CDMP1*^{C400Y} transfected cells contained the unprocessed protein, there was no evidence of cleavage or secretion (Fig. 4*a*).

The apparent inability of CDMP-1^{C400Y} to be processed or secreted suggests that it should have no biological activity. To test this hypothesis, we established an *in vitro* assay to measure BMP activity. The assay was based on the observation that addition of recombinant CDMP-1 or OP-1 to the murine embryonic carcinoma cell line ATDC5 produces an increase in alkaline phosphatase

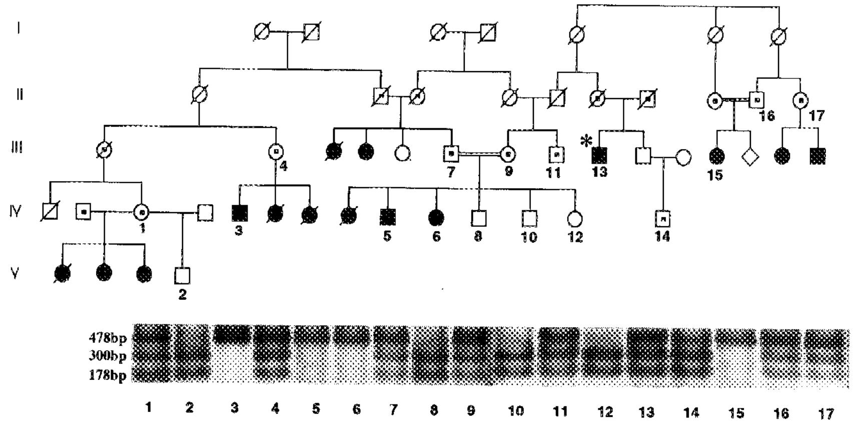

Fig. 2 Pedigree and allele-specific PCR analysis of chondrodysplasia Grebe-type family. We identified twenty individuals with CGT, all members of the original families from the state of Bahía in Brazil described by Quelce-Salgado[12]. Ten of these were re-studied; seven belonged to five sibships in a single kindred, while the others were divided among three seemingly unrelated families (not shown). Affected individuals are indicated by a black box, and heterozygous carriers are represented by a dot in the center of an open box. Numbers refer to family members analysed by PCR, and an asterisk indicates the individual found to be a compound heterozygote. Below the pedigree are *Pst*I digests of 503-bp PCR fragments flanking the mutation site. The G1199A transition (see below) destroys a *Pst*I site. Homozygotes for the G→A transition give a single PCR product of 478 bp, whereas the PCR product from homozygous normal individuals is completely digested to release fragments of 300 bp and 178 bp. All three products are present in digests from heterozygous individuals.

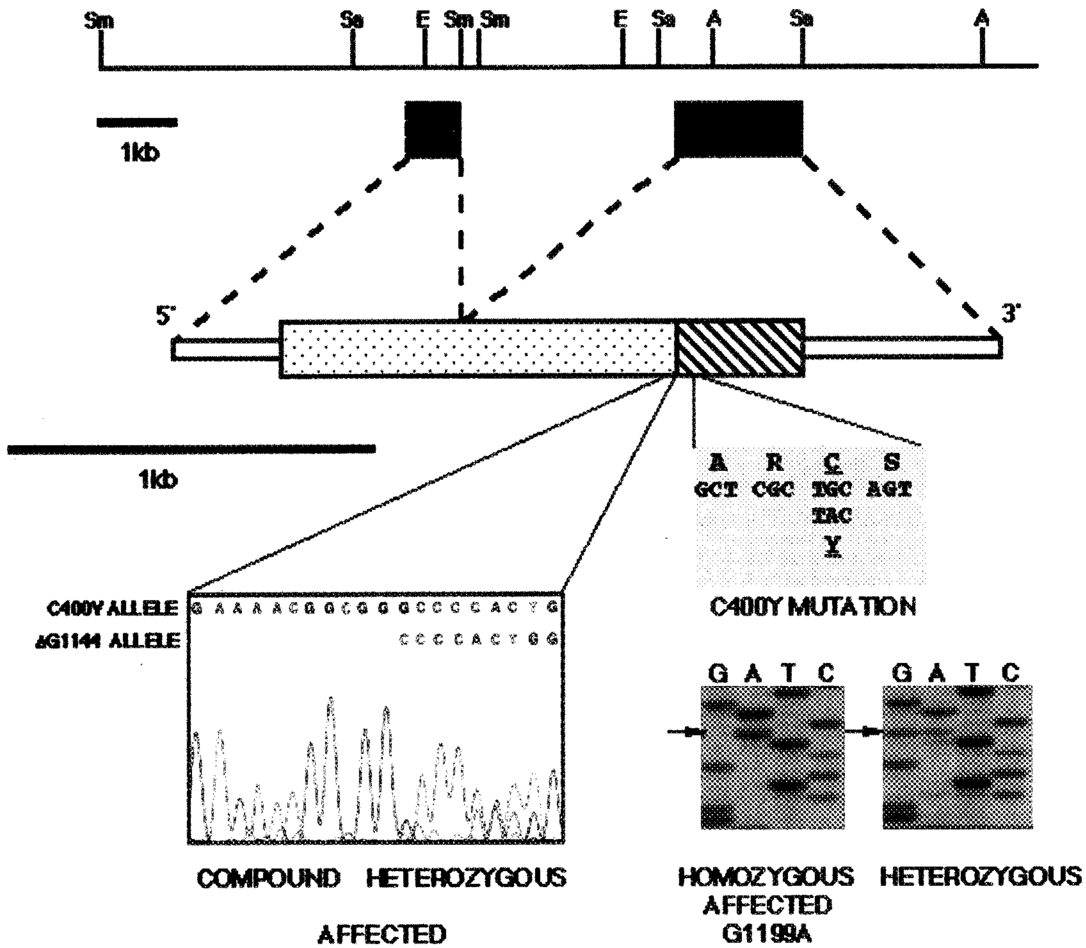

Fig. 3 Affected individuals with CGT harbour the *CDMP1* mutation G1199A, resulting in a C400Y amino-acid change. Partial restriction map (S, *Sac*I; Sm, *Sma*I; A, *Apa*I; E, *Eco*RI) and schematic representation of *CDMP1* showing the exon–intron boundaries, and the domain structure of the derived cDNA. The open reading frame (ORF) of *CDMP1* is encoded by two exons. One exon encodes 5′–untranslated region (UTR), the signal peptide and part of the pro-region. The second exon encodes the remaining part of the pro-region, the mature region (shaded box) and the 3′–UTR. The position and sequence of the G1199A transition within the biologically active mature region, resulting in a C400Y amino-acid change, is shown. Automated sequencing data are presented to demonstrate the ΔG1144 deletion in the compound heterozygote (#13 in Fig. 2).

(AP) activity in a dose- and time-dependent manner. We used this phenomenon to measure BMP activity in ATDC-5 cells transfected with either *CDMP1* or *CDMP1*^{C400Y}. When *CDMP1* was transfected into ATDC5 cells, AP activity was markedly upregulated. In contrast, in *CDMP1*^{C400Y}-transfected cultures, AP activity was found to be at or below the level of those transfected with control plasmid (Fig. 4*b*).

CDMP-1^{C400Y} has a dominant negative effect

We have previously shown that the absence of CDMP-1 results in the clinically milder phenotype of Hunter-Thompson chondrodysplasia[9]. Consequently, loss of function of CDMP-1^{C400Y} alone does not explain the greater severity observed in CGT. As CDMP-1^{C400Y} does not appear to be secreted, it may exert a dominant negative effect by interfering, intracellularly, with the synthesis or secretion of other BMP family members. To address this question, we conducted a number of co-transfection experiments (Figs 4*a*, 5*a–e*). COS-7 cells were co-transfected with *CDMP1*^{C400Y} and *CDMP1*, *BMP2*, *BMP3*, *OP1*, the activin gene or an unrelated gene (*Frzb*). At ratios of 4:1, CDMP-1^{C400Y} inhibited the secretion of CDMP-1 (Fig. 4*a*), OP-1, BMP-2 and BMP-3 (Fig. 5*a,c,d*), but not of the more distantly related family member activin (Fig. 5*e*) or the unrelated protein Frzb (not shown). The association of inhibition of BMP secretion with reduced biological activity was demonstrated in the ATDC-5 cell assay. Cultures co-transfected with *CDMP1*^{C400Y} and *OP1*, at a 4:1 ratio, produced markedly lower levels of AP activity than cultures co-transfected with *OP1* and either *CDMP-1* or control plasmid (Fig. 5*b*). A second finding was that cultures co-transfected with *OP1* and wild-type *CDMP1* produced significantly lower AP levels than those co-transfected with *OP1* and control plasmid. This result provides the basis for further ongoing studies on the biological implications of *BMP* co-expression both *in vivo* and *in vitro*.

CDMP-1 and CDMP-1^{C400Y} can form heterodimers with other BMP family members

To address the possibility that CDMP-1^{C400Y} could form heterodimers with other BMPs, a number of co-immunoprecipitation experiments were performed in transfected COS-7 cells. In preliminary experiments, we demonstrated that BMP-2 and OP-1 can be co-immunoprecipitated from transiently transfected culture supernatants (not shown). Subsequently, COS-7 cells were transfected with expression vectors containing *CDMP1* or *CDMP1*^{C400Y} and *BMP2*, *BMP3*, *OP1* or the activin gene at a 1:1 ratio. Rabbit polyclonal antibodies specifically recognizing native BMP-2, BMP-3, OP-1 or activin were used to immunoprecipitate cell extracts or culture supernatants. Subsequent immunoblot analysis of culture supernatants with mouse myc-tag antibody

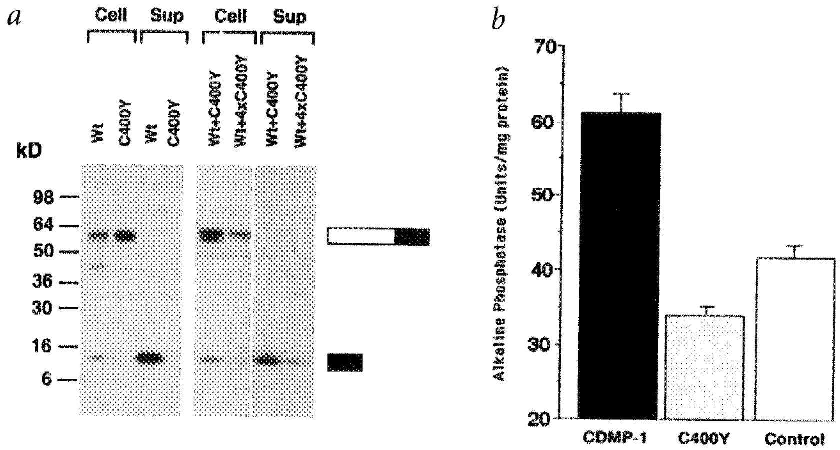

Fig. 4 CDMP-1^{C400Y} is not secreted, is inactive and suppresses the secretion of wild-type CDMP-1. ***a***, Western analyses of COS-7 cell extracts (cell) and media supernatants (sup) from cultures transfected or co-transfected with expression vector pcDNA3 containing the inserts: wt (wild-type *CDMP1*$^{myc\text{-}tag}$) and C400Y (*CDMP1*$^{C400Ymyc\text{-}tag}$). All samples were separated on 4-20% Tris-glycine gels under reducing conditions and analysed with mouse myc-tag monoclonal antibody (9E10). Analysis of cell extracts show that both CDMP-1 and CDMP-1^{C400Y} are synthesized as 56-kD pro-forms, but only CDMP-1 is processed to a 14-kD mature form. In the supernatant, only the mature form of CDMP-1 is secreted. Secretion of CDMP-1 is reduced by the presence of 4× C400Y. The positions of the pro- and mature forms are diagrammatically illustrated adjacent to immunoblot. ***b***, Histogram showing alkaline phosphatase (AP) activity in cell extracts from the osteoprogenitor cell line ATDC-5 transfected with *CDMP1*, *CDMP1*^{C400Y} or the β-galactosidase gene (control). CDMP-1 produces an increase in AP activity; CDMP-1^{C400Y} is inactive. The values represent the means and standard deviations from triplicate cultures.

(9E10) specific for CDMP-1 demonstrated co-immunoprecipitation of CDMP-1 with BMP-2, BMP-3 or OP-1 (Fig. 6, lanes 1–3) but not activin (data not shown). Determining whether CDMP-1^{C400Y} can heterodimerize required immunoprecipitating cell extracts, as CDMP-1^{C400Y} is not secreted. Analysis of cell extracts with affinity-purified peptide antibodies raised in chicken demonstrated the co-immunoprecipitation of BMP-2 and CDMP-1^{C400Y} (Fig. 6, lane 5).

CGT is caused by a mutation in *CDMP1*

Identification of *CDMP1*^{C400Y} as the causative mutation of CGT provides further insight into the role of CDMP-1 and related BMPs during appendicular skeletal morphogenesis. The C400Y mutation substitutes a tyrosine for the first of seven highly conserved cysteine residues in the mature, active protein. The number and spacing of the cysteines are conserved throughout the TGF-β superfamily, enabling the protein to fold into a characteristic cys-

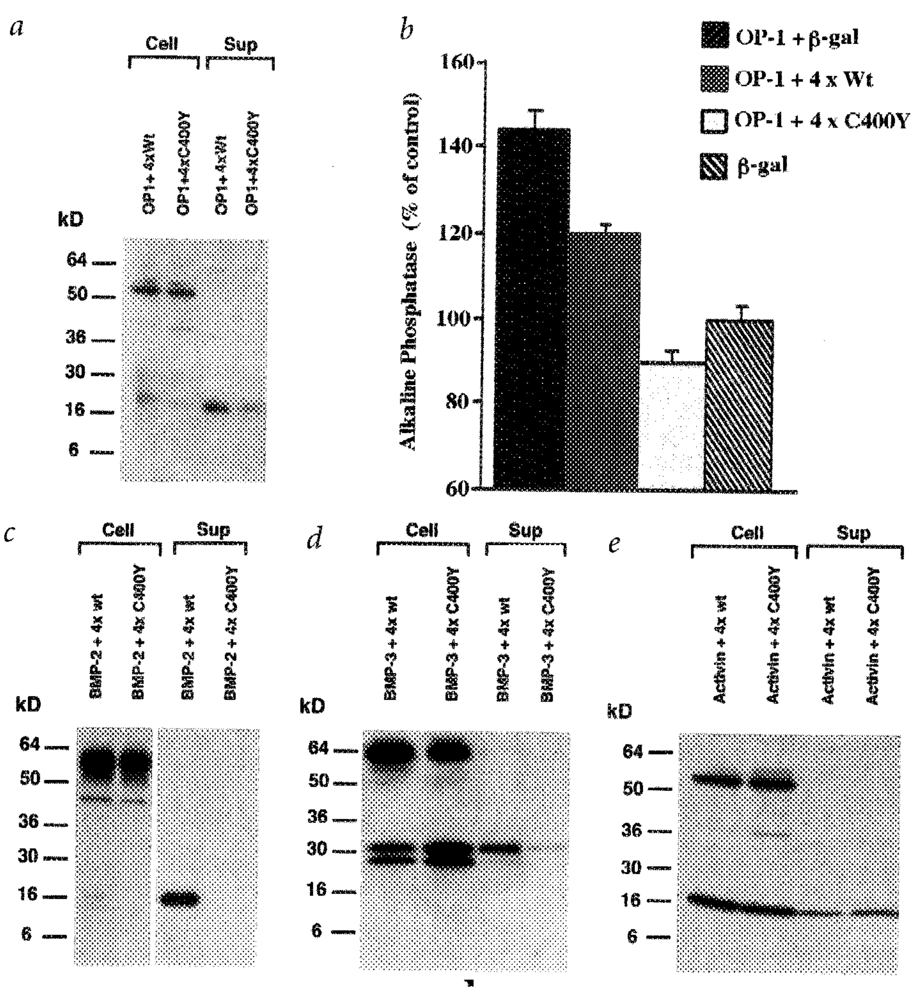

Fig. 5 CDMP-1^{C400Y} can produce a dominant negative effect by inhibiting the secretion of other BMPs. ***a,c–e***, Western analyses of COS-7 cell extracts (cell) and media supernatants (sup) from cultures co-transfected with expression vector pcDNA3 containing either wild-type *CDMP1* (wt) or *CDMP1*^{C400Y} and *OP1*, *BMP2*, *BMP3* or the activin gene. All samples were separated as before and analysed with antibodies specific for (*a*) OP-1 (*b*) BMP-2 (*c*) BMP-3 and (*d*) activin. At a ratio of 4:1, CDMP-1^{C400Y} inhibits the secretion of OP-1, BMP-2 and BMP-3, but not activin. The molecular weights of pro- and mature forms, respectively, are OP-1, 50 kD and 18 kD; BMP-2, 60 kD (not shown) and 16 kD; BMP-3, 64 kD, two bands at 30 and 28 kD; and activin, 58 kD and 14 kD. ***b***, Histogram showing alkaline phosphatase (AP) activity in cell extracts from the osteoprogenitor cell line ATDC-5, co-transfected with *OP1* and *CDMP1*, *CDMP1*^{C400Y} or the β-galactosidase gene (control) at a 1:4 ratio. The presence of CDMP-1^{C400Y} produces a marked reduction in AP activity. The values represent the means and standard deviations from triplicate cultures.

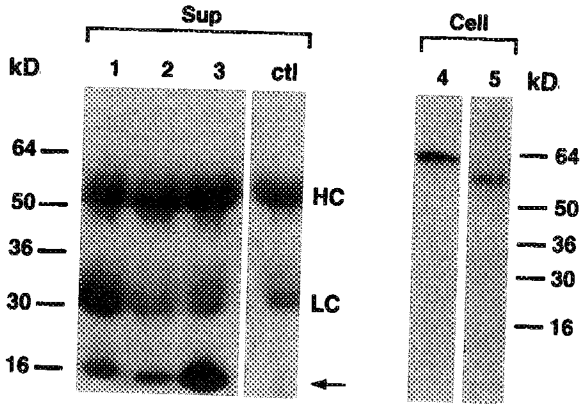

Fig. 6 CDMP-1 and CDMP-1^{C400Y} can form heterodimers with other BMPs. Culture supernatants (lanes 1–3) or cell extracts (lanes 4,5) from COS-7 cells co-transfected with *CDMP1/BMP3* (lane 1), *CDMP1/OP1* (lane 2), *CDMP1/BMP2* (lane 3), *CDMP1/BMP3* (control), *BMP2/OP1* (lane 4) and *CDMP1*^{C400Y}*/OP1* (lane 5). Immunoprecipitation was performed with rabbit antisera (lanes 1–3 and control) specific for BMP-3 (lane 1), OP-1 (lane 2) and BMP-2 (lane 3 and control) or with an OP-1 specific chicken antibody (lanes 4,5). Western analysis was performed using the myc-tag antibody (lanes 1,2,3, control and 5) or a BMP-2-specific rabbit polyclonal antibody (lane 4). The presence of heterodimers is demonstrated by the co-immunoprecipitation of the secreted mature form of CDMP-1 (arrow, lanes 1–3) or the intracellular pro-forms of BMP-2 (lane 4) and CDMP-1^{C400Y} (lane 5). HC and LC indicate the positions of immunoglobulin heavy and light chains, which show non-specific cross-reactivity.

teine knot structure[13–15]. The absence of the first cysteine in CDMP-1^{C400Y} dramatically reduces its processing and secretion. Although the ultimate form of the mutant protein is unknown, its inability to progress through the secretory pathway will presumably lead to its intracellular destruction[16].

CDMP1^{C400Y} mutation may act by selective heterodimerization

One of the most intriguing aspects of CGT is the severity of the phenotype. In a previous study, we identified a null mutation in *CDMP1* as the cause of a clinically milder disorder, chondrodysplasia Hunter-Thompson type[9]. Comparison of the two disorders, together with the mild heterozygous phenotype in CGT (Fig. 1*c–f*), introduces the possibility that the C400Y mutation causes a dominant negative effect. The demonstration that CDMP-1^{C400Y} appears not to be secreted makes it unlikely that it acts at the receptor level. Furthermore, the ability of CDMP-1^{C400Y} to suppress the secretion of only certain members of the TGF-β superfamily suggests that the dominant negative effect is selective, and that a non-specific inhibition of protein secretion is unlikely. Similar studies on TGF-β1 have shown that mutations in the precursor form inhibit the secretion of TGF-β1, -2 and -3 but not BMP-6 (ref. 17). Likewise, mutation of the R-X-X-R cleavage site of *Xenopus* BMP-4 (xBMP-4) inhibits the cleavage of normal xBMP-4 and xBMP-7 but not activin[18].

How could a mutation in one BMP-like molecule selectively affect the secretion of other family members? One possibility is through the formation of non-functional heterodimers. BMPs are usually considered to be homodimers, although heterodimers of BMP-2 and OP-1 have been produced *in vitro*[19,20], and their occurrence *in vivo* has been postulated but not proved[4]. We demonstrate that CDMP-1 is able to heterodimerize with BMP-2, BMP-3 and OP-1, and that the heterodimers are secreted. In contrast, whereas CDMP-1^{C400Y} can form heterodimers intracellularly, there is no evidence for their secretion. Therefore, BMP/CDMP-1^{C400Y} heterodimers will most probably be non-functional. The mode of action of the dominant negative *CDMP1*^{C400Y} mutation is schematically represented in Fig. 7. The potency of the *CDMP1*^{C400Y} mutation in disrupting the function of other BMPs is evident from the individual found to be a compound heterozygote. In this case, where there is one null allele and one *CDMP1*^{C400Y} allele, the phenotype is indistinguishable from affected homozygotes. This implies that if both alleles are expressed equally, half the amount of CDMP-1^{C400Y} can produce the same phenotypic effect.

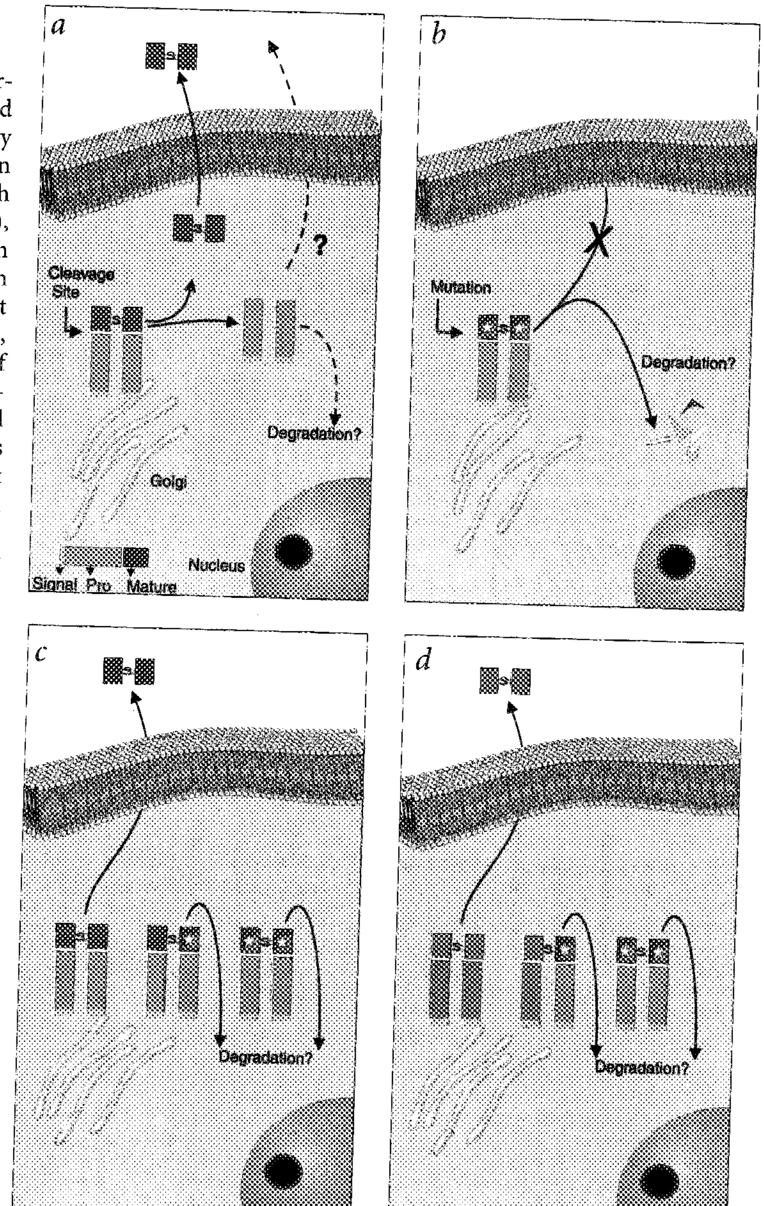

Fig. 7 Diagrammatic representation of proposed mechanism of action of the dominant negative *CDMP-1*^{C400Y} mutation. ***a***, Wild-type (wt) CDMP-1 synthesis and secretion. ***b***, CDMP-1^{C400Y} is synthesized but is not processed or secreted. **c**, CDMP-1^{C400Y} inhibits the processing and thereby the secretion of wild-type CDMP-1. ***d***, CDMP-1^{C400Y} inhibits the processing and secretion of related BMPs by the formation of non-functional heterodimers.

An alternative explanation would be that the absence of secreted wild-type CDMP-1 results in an upregulation of CDMP-1^{C400Y} by means of a compensatory feedback loop mechanism.

CDMP1 expression and limb development

It is known that a number of *BMPs*, including *bmp2, 4, 6, 7(OP1), CDMP1* and *CDMP2* (refs 6–8,21,22), are expressed during limb development, but information on the temporal and spatial patterns of *BMP* co-expression is limited[23]. As our proposed mechanism of action of *CDMP1*^{C400Y} requires its co-expression with other *BMPs*, it is very likely that *CDMP1* is co-expressed with other *BMPs* at some time during limb development. It has been postulated that overlapping expression patterns of different *BMPs* may provide a degree of biological redundancy[24]. In the *BMP7* knockout mouse, morphological abnormalities are restricted to cell populations exclusively expressing *bmp-7*, whereas those shown to be co-expressing other *BMPs* are less affected or are normal[25]. We can extend this principle to explain the differences observed in the two human disorders involving mutations in *CDMP1*. In Hunter-Thompson chondrodysplasia, the absence of CDMP-1 may be partly compensated by the expression of other *BMPs* in the cells where they are normally co-expressed. Conversely, in CGT, the absence of CDMP-1 in conjunction with reduced secretion of other BMPs leads to a greater disruption of skeletogenesis.

During development, ossification of skeletal elements progresses in a proximal-distal direction[26,27]. The severity of skeletal defects observed in both Grebe and Hunter-Thompson chondrodysplasia progresses in the same manner. So far, however, there has been no evidence for a proximal-distal gradient of *CDMP 1* or other *BMP* transcripts during limb development. Our *in-vitro* transfection experiments indicate that secretion of other BMPs is inhibited only by the presence of relatively elevated levels of CDMP-1^{C400Y}. If this is also true *in vivo*, any detrimental effects may occur only when *CDMP1* is normally expressed as the predominant *BMP*-like gene. It remains to be established whether *CDMP1* is the predominant BMP-like gene expressed in the more distal parts of the developing appendicular skeleton.

Brachydactyly in heterozygous individuals

We noted the occurrence of brachydactyly as a common feature of individuals heterozygous for *CDMP1*^{C400Y}. The inherited brachydactylies are a well-documented and classified group of autosomal dominant disorders[28,29], but a genetic link has remained elusive[30]. Brachydactyly has been noted in heterozygotes from a number of other CGT families[31–33], and the heterozygotes observed in the present investigation have phenotypes resembling brachydactyly types A-1, A-4 and C. As part of an independent investigation, we have identified mutations in *CDMP1* in four unrelated families with brachydactyly type C (Polinkovsky *et al.*, unpublished observations). Therefore, heterozygous expression of certain *CDMP1* mutations can lead to haploinsufficiency, producing distinct mild phenotypes. This introduces the concept that heterozygous expression of mutations in other *BMP* genes may cause autosomal dominant traits affecting the development of various organ systems.

Methods

Haplotype analysis and mutation detection. Eight affected individuals and sixteen family members, including nine obligate carriers, agreed to have blood drawn for molecular studies. Fifteen members (eight affected, seven obligate heterozygotes) consented to clinical examination, and X-ray analysis was performed on twelve. Individuals were genotyped for polymorphic (CA)n repeat markers for the loci *D10S195* and *D10S191* and for a *CDMP1*–specific polymorphic (CA)n repeat marker[12]. DNA was isolated from whole blood (QIAmp blood kit, Qiagen) for PCR amplification or was amplified directly from 1-mm blood spots after a brief methanol wash. Primer sets were used to amplify the entire open reading frame (ORF) and exon–intron boundaries as previously described[9]. PCR products were cycle sequenced with [35S]dATP and the AmpliTaq kit (Perkin Elmer), or analysed by automated sequencing (Applied Biosystems model 370A). Familial analysis of the G1199A mutation was performed by digestion of a 503-bp PCR product flanking the mutation region with *Pst*I, followed by analysis on 2.5% agarose gels. The PCR product contains two *Pst*I sites (at nt 300 and 478), but the one at nt 300 is destroyed by the mutation.

Construction of expression vectors. To create a cDNA encoding the complete ORF of wt *CDMP1*, a 1,549-bp *Xba*I/*Hin*dIII fragment encoding the near full-length ORF and 128 bp of the 3′ untranslated region[7] were subcloned into pBluescript (Stratagene). The remaining ORF and 28 bp upstream of the translation initiation codon were generated by PCR of genomic DNA. The PCR product was sequenced and subcloned into the pBluescript vector containing the remaining ORF. The C400Y mutation was introduced by digesting wild-type *CDMP1* with *Afl*II/*Pst*I and replacing the resultant fragment with an *Afl*II/*Pst*I-digested PCR product generated from an affected individual. The full-length wild-type *CDMP1* and *CDMP1*^{C400Y} were subcloned into the eukaryotic vectors pcDNA3.1/Neo(–) and pcDNA3.1/Zeo(–) (Invitrogen). To improve processing efficiency, the pro-region of *CDMP1* was substituted with that of dorsalin. In addition, a myc-tag sequence was substituted into the mature region of *CDMP1* at a location before the first cysteine. Constructs containing the mature regions of wild-type *CDMP1* and *CDMP1*^{C400Y}, coupled to a dorsalin pro-region and a myc epitope, were produced as follows. The plasmid pMT21-BMP-4-mycS[34] was digested with *Eco*RV/ *Xho*I to release the *BMP4* mature region before subcloning PCR-generated mature regions of wild-type *CDMP1* and *CDMP1*^{C400Y}. Full-length human cDNAs for *BMP2* and *OP1* (Creative BioMolecules), *BMP3* (from W. Wood, Genentech) and activin (provided by D. Huylebroeck, VIB) were subcloned into pcDNA3.1/Zeo(–). The pSV-β–galactosidase vector (Promega) was used to monitor transfection efficiency.

Transfections. COS-7 cells were maintained in Opti-MEM (modified Eagle's medium) I (Life Technologies) supplemented with 5% fetal bovine serum (Collaborative Research) and antibiotics (100 U/ml penicillin, 100 μg/ml streptomycin and 250 ng/ml amphotericin B (Gibco BRL)). The cell line ATDC5, derived from murine embryonic carcinoma cells[35], was provided by P.V. Hauschka (Children's Hospital Medical Center, Boston) and maintained in 1:1 mixture of Dulbecco's MEM and Ham's F-12 (Life Technologies) with the same supplements as above. Both cell lines were incubated at 37 °C in an atmosphere containing 5% CO_2. Cells were plated at approximately 60% confluence in 100-mm dishes and transfected 24 h later with 5 μl/ml Lipofectamine (Life Technologies) and 1–5 μg/ml DNA in Opti-MEM I according to the manufacturer's instructions. After transfection, COS-7 cells were maintained in Opti-MEM1 and antibiotics for 2 days, and ATDC5 cells were maintained in a chemically defined basal medium (Erlacher *et al.*, unpublished observations) for 4 days before analysis.

Western analysis. Whole-cell lysates were extracted in RIPA buffer (150 mM NaCl, 1% NonIdet P-40, 0.5% deoxycholate, 0.1% SDS, 50 mM Tris, pH 8), separated on 4–20% Tris-glycine polyacrylamide gels (Novex) and transferred to Immobilon (Millipore) PVDF membrane with a GENIE electrophoretic blotter (Idea Scientific Company). Membranes were incubated in blocking solution (10 mM Tris pH 7.5, 150 mM NaCl, 0.1% Tween 20, 4% BSA) for 1 h before incubation with primary antibody. Mouse anti-c-myc monoclonal antibody 9E10 (Santa Cruz Biotech) and rabbit polyclonal antisera specific for OP-1, BMP-2 (Creative BioMolecules) and activin (provided by W. Vale, Salk Institute for Biological Studies) were used at a 1/1,000 dilution. Chicken polyclonal, affinity-purified peptide, antisera specific for OP-1 and BMP-2 (Pfizer) were used at a 1/500 dilution, and the rabbit polyclonal antiserum, FS-3 (ref. 36), specific for BMP-3, was used at a 1/2,000 dilution. All primary antisera were diluted in TBST (10 mM Tris pH 7.9, 150 mM NaCl 0.1% Tween 20) and 0.4% BSA, and incubated with pre-blocked membranes at room temperature for 1 h. The membranes were washed three times in TBST and incubated with horse-radish peroxidase–conjugated secondary antibody (Jackson Laboratories), at a 1/20,000 dilution, for 1 h. Immunoreactive proteins were detected with the SuperSignal chemiluminescent system (Pierce).

Immunoprecipitation. Rabbit and chicken antisera (50 μl) were incubated at 4 °C (with rotation) overnight with protein A–agarose and protein

G–agarose (Boehringer Mannheim) respectively in 450 μl of 150 mM NaCl, 50 mM Tris-HCl pH 7.4. Cell extracts or culture supernatants (100–400 μl) and RIPA buffer (0–400 μl) were added, and incubation continued for 1 h. The samples were centrifuged at 3,000 rpm for 1 min and washed twice in 150 mM NaCl, 50 mM Tris-HCl pH 7.4, once in 500 mM NaCl, 50 mM Tris-HCl pH 7.4 and once in 50 mM Tris-HCl pH 7.4. The pellets were re-suspended in 50 μl of 2× Laemmli sample buffer and 4% β-mercaptoethanol and boiled. Electrophoresis on 4–20% Tris-glycine gels, transfer to Immobilon PVDF membrane and western analysis were performed as before.

Alkaline phosphatase assay. Cells were washed with phosphate-buffered saline (PBS) and extracted by brief sonication in PBS containing 0.05% Triton X-100. Alkaline phosphatase enzymatic activity was assayed in 3.5 mM *p*-nitrophenyl phosphate (PNP), 50 mM sodium barbital pH 9.3 for 30 min at room temperature. The reaction was stopped with 0.5 M NaOH, and absorbance was measured at 400 nm. The protein content of each sample was determined with the Bradford protein assay (BIO-RAD). Alkaline phosphatase activity was calculated as μmol PNP produced/min/mg protein.

Acknowledgements
We wish to thank G. Ramsby and J. Soares Filho for help in interpreting skeletal X-rays; F. Cassia and J. Correa Neto for assisting in the clinical evaluation of the families; and A. Quelce-Salgado for helping us in the initial stages of the work. We are grateful to M. Moos, Jr., M. Kuehn, P. Gehron-Robey and M. Warman for their useful suggestions, to J. Aarons for graphic illustration and M. Nandedkar for editorial assitance. This work was supported in part by grants HD-22610 and the Coles Family Foundation (to P.T.).

Received 14 April; accepted 14 July 1997.

1. Hall, B.K. Embryonic bone formation with special reference to epithelial-mesenchymal interactions and growth factors. in *Bone: A Treatise*. vol. 8, *Mechanisms of Bone Development and Growth* (ed. Hall, B.K.) 137–192 (CRC Press, Boca Raton, Florida,1994).
2. Wozney, J.M. *et al.* Novel regulators of bone formation: molecular clones and activities. *Science* **242**, 1528–1534 (1988).
3. Luyten, F.P. *et al.* Purification and partial amino acid sequence of osteogenin, a protein initiating bone differentiation. *J. Biol. Chem.* **264**, 13377–13380 (1989).
4. Sampath, T.K. *et al.* Bovine osteogenic protein is composed of dimers of OP-1 and BMP-2A, two members of the transforming growth factor β superfamily. *J. Biol. Chem.* **265**, 13198–13205 (1990).
5. Hogan, B.L.M. Bone morphogenetic proteins: multifunctional regulators of vertebrate development. *Genes Dev.* **10**, 1580–1594 (1996).
6. Chang, S.C. *et al.* Cartilage-derived morphogenetic proteins: new members of the transforming growth factor–β superfamily predominantly expressed in long bones during human embryonic development. *J. Biol. Chem.* **269**, 28227–28234 (1994).
7. Storm, E.E. *et al.* Limb alterations in *brachypodism* mice due to mutations in a new member of the TGFβ-superfamily. *Nature* **368**, 639–643 (1994).
8. Storm, E.E. & Kingsley, D.M. Joint patterning defects caused by single and double mutations in members of the bone morphogenetic protein (BMP) family. *Development* **122**, 3969–3979 (1996).
9. Thomas, J.T. *et al.* A human chondrodysplasia due to a mutation in a TGF-β superfamily member. *Nature Genet.* **12**, 315–317 (1996).
10. Grebe, H. Die Achondrogenesis: ein Einfach rezessives Erbmerkmal. *Folia Hered. Pathol.* **2**, 23–29 (1952).
11. Quelce-Salgado, A. A new type of dwarfism with various bone aplasias and hypoplasias of the extremities. *Acta Genet.* **14**, 63–66 (1964).
12. Lin, K., Thomas, J.T., McBride, O.W. & Luyten, F.P. Assignment of a new TGF-β superfamily member, human cartilage-derived morphogenetic protein–1, to chromosome 20q11.2. *Genomics* **34**, 150–151 (1996).
13. Daopin, S., Piez, K., Ogawa, Y. & Davies, D.R. Crystal structure of transforming growth factor–β2: an unusual fold for the superfamily. *Science* **257**, 369–373 (1992).
14. Venkataraman, G., Sasisekharan, V., Cooney, C.L., Langer, R., & Sasisekharan, R. Complex flexability of the transforming growth factor β superfamily. *Proc. Natl. Acad. Sci. USA* **92**, 5406–5410 (1995).
15. Griffith, D.L., Keck, P.C., Sampath, T.K., Rueger, D.C. & Carlson, W.D. Three-dimensional structure of recombinant human osteogenic protein-1: structural paradigm for the transforming growth factor β superfamily. *Proc. Natl. Acad. Sci. USA* **93**, 878–883 (1996).
16. Kopito, R.R. ER quality control: the cytoplasmic connection. *Cell* **88**, 427–430 (1997).
17. Lopez, A.R., Cook, J., Deininger, P.L. & Derynck, R. Dominant negative mutants of transforming growth factor–beta 1 inhibit the secretion of different transforming growth factor–beta isoforms. *Mol. Cell. Biol.* **12**, 1674–1679 (1992).
18. Hawley, S.H.B. *et al.* Disruption of BMP signals in embryonic xenopus ectoderm leads to direct neural induction. *Genes Dev.* **9**, 2923–2935 (1995).
19. Aono, A. *et al.* Potent ectopic bone-inducing activity of bone morphogenetic protein-4/7 heterodimer. *Biochem. Biophys. Res. Commun.* **210**, 670–677 (1995).
20. Israel, D.I. *et al.* Heterodimeric bone morphogenetic proteins show enhanced activty invitro and in vivo. *Growth Factors* **13**, 291–300 (1996).
21. Jones, C.M., Lyons, K.M. & Hogan, B.L.M. Involvement of bone morphogenetic protein-4 (*BMP-4*) and *Vgr-1* in morphogenesis and neurogenesis in the mouse. *Development* **111**, 531–542 (1991).
22. Luo, G. *et al.* BMP-7 is an inducer of nephrogenesis, and is also required for eye development and skeletal patterning. *Genes Dev.* **9**, 2808–2820 (1995).
23. Lyons, K.M., Hogan, B.L.M. & Robertson, E.J. Colocalization of BMP-7 and BMP-2 mRNAs suggests that these factors cooperatively mediate tissue interactions during murine development. *Mech. Dev.* **50**, 71–78 (1995).
24. Kingsley, D.M. What do BMPs do in mammals? Clues from the mouse short-ear mutation. *Trends Genet.* **10**, 16–21 (1994).
25. Dudley, A.T. & Robertson, E.J. Overlapping expression domains of bone morphogenetic protein family members potentially account for limited tissue defects in BMP-7 deficient embryos. *Dev. Dynamics* **208**, 349–362 (1997)
26. Saunders, J.W. The proximo-distal sequence of origin of the parts of the chick wing and the role of the ectoderm. *J. Exp. Zool.* **108**, 363–404 (1948).
27. Gray, D.J., Gardner, E. & O'Rahilly, R. The prenatal development of the skeleton and joints of the human hand. *Am. J. Anat.* **101**, 169–223 (1957).
28. Bell, J. On brachydactyly and symphalangism. *Treas. Hum. Inherit.* **5**, 1–30 (1951).
29. Fitch, N. Classification and identification of inherited brachydactylies. *J. Med. Genet.* **16**, 36–44 (1978).
30. Mastrobattista, J.M., Dolle, P., Blanton, S.H. & Northrup, H. Evaluation of candidate genes for familial brachydactyly. *J. Med. Genet.* **32**, 851–854 (1995).
31. Kumar, D., Curtis, D. & Blank, C.E. Grebe chondrodysplasia and brachydactyly in a family. *Clin. Genet.* **25**, 68–72 (1984).
32. Feng, B., Chen, R., Luo, J., Chen, R. & Zheng, Y. A kindred of Miao nationality affected with Grebe–Quelce-Salgado achondrogenesis. *Acta Genet. Sin.* **12**, 378–386 (1985).
33. Garcia-Castro, J.M. & Perez-Comas, A. Non-lthal achondrogenesis (Grebe–Quelce-Salgado type) in two Puerto Rican sibships. *J. Pediatr.* **87**, 948–952 (1975).
34. Zimmerman L.B., De Jesus-Escobar, J.M. & Harland, R.M. The Spemann organizer signal noggin binds and inactivates bone morphogenetic protein 4. *Cell* **86**, 599–606 (1996).
35. Atsumi, T., Miwa, Y., Kimata, K. & Ikawa, Y. A chondrogenic cell line derived from a differentiating culture of AT805 teratocarcinoma cells. *Cell Differ. Dev.* **30**, 109–116 (1990).
36. Vukicevic, S., Helder, M.N. & Luyten, F.P. Developing human lung and kidney are major sites for synthesis of bone morphogenetic protein-3 (osteogenin). *J. Histochem. Cytochem.* **42**, 869–875 (1994).